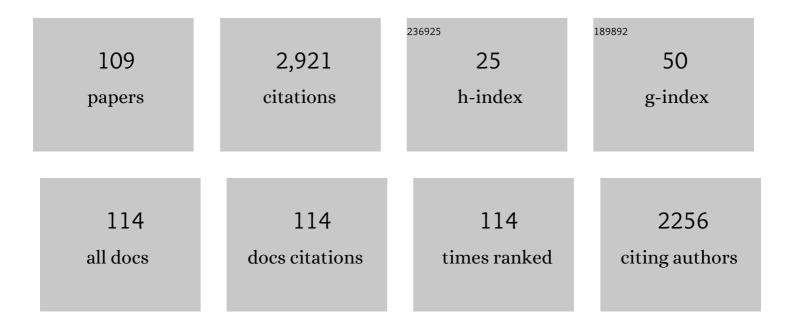
Michele Piana

List of Publications by Year in descending order

Source: https://exaly.com/author-pdf/7995190/publications.pdf Version: 2024-02-01



#	Article	IF	CITATIONS
1	Bad and Good Errors: Value-Weighted Skill Scores in Deep Ensemble Learning. IEEE Transactions on Neural Networks and Learning Systems, 2024, 35, 1993-2002.	11.3	4
2	Longitudinal analysis of atherosclerotic plaques evolution: an 18F-NaF PET/CT study. Journal of Nuclear Cardiology, 2022, 29, 1713-1723.	2.1	8
3	Visibility-Based Imaging Methods. , 2022, , 89-119.		0
4	Application to Solar Flares. , 2022, , 121-139.		0
5	18F-FDG-PET correlates of aging and disease course in ALS as revealed by distinct PVC approaches. European Journal of Radiology Open, 2022, 9, 100394.	1.6	1
6	Opportunistic skeletal muscle metrics as prognostic tools in metastatic castration-resistant prostate cancer patients candidates to receive Radium-223. Annals of Nuclear Medicine, 2022, 36, 373-383.	2.2	6
7	Positron emission tomography and single photon emission computed tomography imaging of tertiary lymphoid structures during the development of lupus nephritis. International Journal of Immunopathology and Pharmacology, 2021, 35, 205873842110336.	2.1	5
8	The flare likelihood and region eruption forecasting (FLARECAST) project: flare forecasting in the big data & machine learning era. Journal of Space Weather and Space Climate, 2021, 11, 39.	3.3	24
9	The Role of Spectral Complexity in Connectivity Estimation. Axioms, 2021, 10, 35.	1.9	6
10	Gain and loss of function mutations in biological chemical reaction networks: a mathematical model with application to colorectal cancer cells. Journal of Mathematical Biology, 2021, 82, 55.	1.9	4
11	The role of endoplasmic reticulum in in vivo cancer FDG kinetics. PLoS ONE, 2021, 16, e0252422.	2.5	4
12	STIX X-ray microflare observations during the Solar Orbiter commissioning phase. Astronomy and Astrophysics, 2021, 656, A4.	5.1	23
13	Flare-forecasting Algorithms Based on High-gradient Polarity Inversion Lines in Active Regions. Astrophysical Journal, 2021, 915, 38.	4.5	13
14	Feature augmentation for the inversion of the Fourier transform with limited data. Inverse Problems, 2021, 37, 105001.	2.0	6
15	Myocardial Metabolic Response Predicts Chemotherapy Curative Potential on Hodgkin Lymphoma: A Proof-of-Concept Study. Biomedicines, 2021, 9, 971.	3.2	1
16	Mathematical Models for FDG Kinetics in Cancer: A Review. Metabolites, 2021, 11, 519.	2.9	2
17	Radiomics and Artificial Intelligence for Outcome Prediction in Multiple Myeloma Patients Undergoing Autologous Transplantation: A Feasibility Study with CT Data. Diagnostics, 2021, 11, 1759.	2.6	10
18	Quantitative Imaging and Radiomics in Multiple Myeloma: A Potential Opportunity?. Medicina (Lithuania), 2021, 57, 94.	2.0	6

#	Article	IF	CITATIONS
19	Visibility Interpolation in Solar Hard X-Ray Imaging: Application to RHESSI and STIX. Astrophysical Journal, 2021, 919, 133.	4.5	6
20	Overview of radiomics in breast cancer diagnosis and prognostication. Breast, 2020, 49, 74-80.	2.2	161
21	Mathematical modelling of nuclear medicine data. , 2020, , .		3
22	Impact of treatment on cellular immunophenotype in MS. Neurology: Neuroimmunology and NeuroInflammation, 2020, 7, .	6.0	17
23	Spinal cord hypermetabolism extends to skeletal muscle in amyotrophic lateral sclerosis: a computational approach to [18F]-fluorodeoxyglucose PET/CT images. EJNMMI Research, 2020, 10, 23.	2.5	17
24	On the two-step estimation of the cross-power spectrum for dynamical linear inverse problems. Inverse Problems, 2020, 36, 045010.	2.0	8
25	MEM_GE: A New Maximum Entropy Method for Image Reconstruction from Solar X-Ray Visibilities. Astrophysical Journal, 2020, 894, 46.	4.5	21
26	A Comparative Study of the Robustness of Frequency-Domain Connectivity Measures to Finite Data Length. Brain Topography, 2019, 32, 675-695.	1.8	17
27	Count-based imaging model for the Spectrometer/Telescope for Imaging X-rays (STIX) in Solar Orbiter. Astronomy and Astrophysics, 2019, 624, A130.	5.1	17
28	Automated Definition of Skeletal Disease Burden in Metastatic Prostate Carcinoma: A 3D Analysis of SPECT/CT Images. Cancers, 2019, 11, 869.	3.7	1
29	G6Pase location in the endoplasmic reticulum: Implications on compartmental analysis of FDG uptake in cancer cells. Scientific Reports, 2019, 9, 2794.	3.3	22
30	Feature Ranking of Active Region Source Properties in Solar Flare Forecasting and the Uncompromised Stochasticity of Flare Occurrence. Astrophysical Journal, 2019, 883, 150.	4.5	43
31	Bayesian multi-dipole modelling in the frequency domain. Journal of Neuroscience Methods, 2019, 312, 27-36.	2.5	8
32	Reference Tissue Models for FDG-PET Data: Identifiability and Solvability. IEEE Transactions on Radiation and Plasma Medical Sciences, 2018, 2, 177-186.	3.7	9
33	A Hybrid Supervised/Unsupervised Machine Learning Approach to Solar Flare Prediction. Astrophysical Journal, 2018, 853, 90.	4.5	50
34	FLARECAST: An I4.0 Technology for Space Weather Using Satellite Data. , 2018, , .		1
35	Effect of starvation on brain glucose metabolism and 18F-2-fluoro-2-deoxyglucose uptake: an experimental in-vivo and ex-vivo study. EJNMMI Research, 2018, 8, 44.	2.5	14
36	Coronal Hard X-Ray Sources Revisited. Astrophysical Journal, 2018, 867, 82.	4.5	14

#	Article	IF	CITATIONS
37	Interplay between spinal cord and cerebral cortex metabolism in amyotrophic lateral sclerosis. Brain, 2018, 141, 2272-2279.	7.6	33
38	Identification of Multiple Hard X-Ray Sources in Solar Flares: A Bayesian Analysis of the 2002 February 20 Event. Astrophysical Journal, 2018, 862, 68.	4.5	9
39	Assessment of Skeletal Tumor Load in Metastasized Castration-Resistant Prostate Cancer Patients: A Review of Available Methods and an Overview on Future Perspectives. Bioengineering, 2018, 5, 58.	3.5	3
40	Machine Learning for Flare Forecasting. , 2018, , 355-364.		6
41	Metabolic and densitometric correlation between atherosclerotic plaque and trabecular bone: an F-Natrium-Fluoride PET/CT study. American Journal of Nuclear Medicine and Molecular Imaging, 2018, 8, 387-396.	1.0	2
42	Functional Activation of Osteoclast Commitment in Chronic Lymphocytic Leukaemia: a Possible Role for RANK/RANKL Pathway. Scientific Reports, 2017, 7, 14159.	3.3	14
43	A physiology-based parametric imaging method for FDC–PET data. Inverse Problems, 2017, 33, 125010.	2.0	12
44	Compressed sensing and finite isotropic wavelets for the STIX reconstruction problem. , 2017, , .		1
45	Tumor Burden and Intraosseous Metabolic Activity as Predictors of Bone Marrow Failure during Radioisotope Therapy in Metastasized Prostate Cancer Patients. BioMed Research International, 2017, 2017, 1-10.	1.9	12
46	Inverse Modeling for MEG/EEG Data. Springer INdAM Series, 2017, , 239-253.	0.5	3
47	Expectation maximization and the retrieval of the atmospheric extinction coefficients by inversion of Raman lidar data. Optics Express, 2016, 24, 21497.	3.4	11
48	A PET/CT approach to spinal cord metabolism in amyotrophic lateral sclerosis. European Journal of Nuclear Medicine and Molecular Imaging, 2016, 43, 2061-2071.	6.4	27
49	HT-BONE: a graphical user interface for the identification of bone profiles in CT images via extended Hough transform. , 2016, , .		3
50	A new compartmental method for the analysis of liver FDG kinetics in small animal models. EJNMMI Research, 2015, 5, 107.	2.5	19
51	Application of Possibilistic C-Means for Fault Detection in Nuclear Power Plant Data. Journal of Engineering for Gas Turbines and Power, 2015, 137, .	1.1	1
52	The Process of Data Formation for the <i>Spectrometer/Telescope for Imaging X-rays (STIX)</i> in <i>Solar Orbiter</i> . SIAM Journal on Imaging Sciences, 2015, 8, 1315-1331.	2.2	11
53	Allogeneic cell transplant expands bone marrow distribution by colonizing previously abandoned areas: an FDG PET/CT analysis. Blood, 2015, 125, 4095-4102.	1.4	23
54	Linear Sampling. , 2015, , 800-804.		0

#	Article	IF	CITATIONS
55	18F-fluorodeoxyglucose PET/CT in aplastic anemia: a literature review and the potential of a computational approach. Clinical Practice (London, England), 2014, 11, 613-621.	0.1	4
56	SYSTEMATIC DE-SATURATION OF IMAGES FROM THE ATMOSPHERIC IMAGING ASSEMBLY IN THE <i>SOLAR DYNAMICS OBSERVATORY</i> . Astrophysical Journal Letters, 2014, 793, L23.	8.3	12
57	Regularization of multiplicative iterative algorithms with nonnegative constraint. Inverse Problems, 2014, 30, 035012.	2.0	11
58	Adult Advanced Chronic Lymphocytic Leukemia: Computational Analysis of Whole-Body CT Documents a Bone Structure Alteration. Radiology, 2014, 271, 805-813.	7.3	24
59	Application of the Inhomogeneous LippmannSchwinger Equation to Inverse Scattering Problems. SIAM Journal on Applied Mathematics, 2013, 73, 212-231.	1.8	16
60	An optimisation approach to multiprobe cryosurgery planning. Computer Methods in Biomechanics and Biomedical Engineering, 2013, 16, 885-895.	1.6	21
61	The Use of Electron Maps to Constrain Some Physical Properties of Solar Flares. Solar Physics, 2013, 283, 177-186.	2.5	3
62	Metformin Temporal and Localized Effects on Gut Glucose Metabolism Assessed Using ¹⁸ F-FDG PET in Mice. Journal of Nuclear Medicine, 2013, 54, 259-266.	5.0	50
63	Hough Transform of Special Classes of Curves. SIAM Journal on Imaging Sciences, 2013, 6, 391-412.	2.2	32
64	RETURN CURRENTS AND ENERGY TRANSPORT IN THE SOLAR FLARING ATMOSPHERE. Astrophysical Journal, 2013, 773, 121.	4.5	8
65	Pattern recognition in medical imaging by means of the Hough transform of curves. , 2013, , .		4
66	THE SPECIFIC ACCELERATION RATE IN LOOP-STRUCTURED SOLAR FLARES—IMPLICATIONS FOR ELECTRON ACCELERATION MODELS. Astrophysical Journal, 2013, 766, 28.	4.5	25
67	Estimate of FDG Excretion by means of Compartmental Analysis and Ant Colony Optimization of Nuclear Medicine Data. Computational and Mathematical Methods in Medicine, 2013, 2013, 1-10.	1.3	10
68	Intrabone Transplant of Cord Blood Stem Cells Establishes a Local Engraftment Store: A Functional PET/FDG Study. Journal of Biomedicine and Biotechnology, 2012, 2012, 1-8.	3.0	8
69	EMPIRICAL DETERMINATION OF THE ENERGY LOSS RATE OF ACCELERATED ELECTRONS IN A WELL-OBSERVED SOLAR FLARE. Astrophysical Journal, 2012, 751, 129.	4.5	9
70	PROPERTIES OF THE ACCELERATION REGIONS IN SEVERAL LOOP-STRUCTURED SOLAR FLARES. Astrophysical Journal, 2012, 755, 32.	4.5	43
71	Estimating the whole bone-marrow asset in humans by a computational approach to integrated PET/CT imaging. European Journal of Nuclear Medicine and Molecular Imaging, 2012, 39, 1326-1338.	6.4	51
72	An interpolation/extrapolation approach to X-ray imaging of solar flares. Inverse Problems and Imaging, 2012, 6, 147-162.	1.1	5

#	Article	IF	CITATIONS
73	Deducing Electron Properties from Hard X-ray Observations. Space Science Reviews, 2011, 159, 301-355.	8.1	143
74	A Visualization Method for Breast Cancer Detection Using Microwaves. SIAM Journal on Applied Mathematics, 2010, 70, 2509-2533.	1.8	11
75	Particle filtering, beamforming and multiple signal classification for the analysis of magnetoencephalography time series: a comparison of algorithms. Inverse Problems and Imaging, 2010, 4, 169-190.	1.1	15
76	HARD X-RAY IMAGING OF SOLAR FLARES USING INTERPOLATED VISIBILITIES. Astrophysical Journal, 2009, 703, 2004-2016.	4.5	37
77	An inverse scattering based hybrid method for the measurement of the complex dielectric permittivities of arbitrarily shaped homogenous targets. , 2009, , .		3
78	Dynamical MEG source modeling with multiâ€ŧarget Bayesian filtering. Human Brain Mapping, 2009, 30, 1911-1921.	3.6	52
79	THE LOCATION OF CENTROIDS IN PHOTON AND ELECTRON MAPS OF SOLAR FLARES. Astrophysical Journal, 2009, 706, 917-922.	4.5	13
80	A Hybrid Approach to 3D Microwave Imaging by Using Linear Sampling and ACO. IEEE Transactions on Antennas and Propagation, 2008, 56, 3224-3232.	5.1	58
81	Postprocessing of the Linear Sampling Method by Means of Deformable Models. SIAM Journal of Scientific Computing, 2008, 30, 2613-2634.	2.8	9
82	A linear sampling approach to crack detection in microwave imaging. , 2008, , .		11
83	Determining the Spatial Variation of Accelerated Electron Spectra in Solar Flares. AIP Conference Proceedings, 2008, , .	0.4	6
84	On the use of the Reciprocity Gap Functional in inverse scattering with near-field data: An application to mammography. Journal of Physics: Conference Series, 2008, 135, 012032.	0.4	2
85	Electron Flux Spectral Imaging of Solar Flares through Regularized Analysis of Hard Xâ€Ray Source Visibilities. Astrophysical Journal, 2007, 665, 846-855.	4.5	56
86	Electronâ€Electron Bremsstrahlung Emission and the Inference of Electron Flux Spectra in Solar Flares. Astrophysical Journal, 2007, 670, 857-861.	4.5	29
87	Particle filters: A new method for reconstructing multiple current dipoles from MEG data. International Congress Series, 2007, 1300, 173-176.	0.2	12
88	Particle filters and RAP-MUSIC in MEG source modelling: A comparison. International Congress Series, 2007, 1300, 161-164.	0.2	3
89	The use of the linear sampling method for obtaining super-resolution effects in Born approximation. Journal of Computational and Applied Mathematics, 2007, 203, 145-158.	2.0	13
90	Modulation of brain and behavioural responses to cognitive visual stimuli with varying signal-to-noise ratios. Clinical Neurophysiology, 2006, 117, 1098-1105.	1.5	13

#	Article	IF	CITATIONS
91	FIST: A fast visualizer for fixed-frequency acoustic and electromagnetic inverse scattering problems. Simulation Modelling Practice and Theory, 2006, 14, 177-187.	3.8	2
92	Regularized Reconstruction of the Differential Emission Measure from Solar Flare Hard X-Ray Spectra. Solar Physics, 2006, 237, 61-83.	2.5	23
93	Evaluation of Algorithms for Reconstructing Electron Spectra from Their Bremsstrahlung Hard Xâ€Ray Spectra. Astrophysical Journal, 2006, 643, 523-531.	4.5	52
94	Determination of Electron Flux Spectra in a Solar Flare with an Augmented Regularization Method: Application to Rhessi Data. Solar Physics, 2005, 226, 317-325.	2.5	42
95	The use of constraints for solving inverse scattering problems: physical optics and the linear sampling method. Inverse Problems, 2005, 21, 207-222.	2.0	11
96	Are Loss Functions All the Same?. Neural Computation, 2004, 16, 1063-1076.	2.2	310
97	Generalized Regularization Techniques with Constraints for the Analysis of Solar Bremsstrahlung X-ray Spectra. Solar Physics, 2004, 225, 293-309.	2.5	48
98	Anisotropic Bremsstrahlung Emission and the Form of Regularized Electron Flux Spectra in Solar Flares. Astrophysical Journal, 2004, 613, 1233-1240.	4.5	48
99	The linear sampling method in inverse electromagnetic scattering theory. Inverse Problems, 2003, 19, S105-S137.	2.0	277
100	Regularized Electron Flux Spectra in the 2002 July 23 Solar Flare. Astrophysical Journal, 2003, 595, L127-L130.	4.5	86
101	Experimental validation of a linear model for data reduction in chirp-pulse microwave CT. IEEE Transactions on Medical Imaging, 2002, 21, 385-395.	8.9	26
102	Numerical validation of the linear sampling method. Inverse Problems, 2002, 18, 511-527.	2.0	39
103	A SIMPLE REGULARIZATION METHOD FOR SOLVING ACOUSTICAL INVERSE SCATTERING PROBLEMS. Journal of Computational Acoustics, 2001, 09, 565-573.	1.0	1
104	Inequalities for inverse scattering problems in absorbing media. Inverse Problems, 2001, 17, 597-605.	2.0	6
105	Role of noise in image processing by the human perceptive system. Physical Review E, 2000, 62, 1104-1109.	2.1	54
106	The simple method for solving the electromagnetic inverse scattering problem: the case of TE polarized waves. Inverse Problems, 1998, 14, 597-614.	2.0	45
107	A simple method using Morozov's discrepancy principle for solving inverse scattering problems. Inverse Problems, 1997, 13, 1477-1493.	2.0	270
108	Thermal bremsstrahlung hard X-rays and primary energy release in flares. Solar Physics, 1995, 156, 315-335.	2.5	13

#	Article	IF	CITATIONS
109	Transfreq: A Python package for computing the thetaâ€ŧoâ€alpha transition frequency from resting state electroencephalographic data. Human Brain Mapping, 0, , .	3.6	1